

# Using Spatial Light Modulators within MIMO Visible Light Communication Receivers to Dynamically Adjust the Optical Channel

Jimmy C. Chau  
Electrical and Computer  
Engineering  
Boston University  
jchau@bu.edu

Cristian Morales  
Electrical and Computer  
Engineering  
Boston University  
crism@bu.edu

Thomas D.C. Little  
Electrical and Computer  
Engineering  
Boston University  
tdcl@bu.edu

## Abstract

In this paper, we propose a new MIMO visible light communication (VLC) receiver architecture that can dynamically adjust the optical channel by using a spatial light modulator (SLM). We also present preliminary operating procedures and control algorithms for this SLM VLC receiver to measure the gain from each transmitter, to configure the SLM, and to track the transmitters as they move relative to the receiver. Through the design of a two-photodetector prototype and simplified models for imaging systems, we demonstrate that the SLM VLC receiver can outperform similar imaging VLC receivers that do not use a SLM, even when the VLC receiver with the SLM is equipped with more photodetectors, in regards to channel matrix rank and condition number.

## Categories and Subject Descriptors

B.4.1 [Input/Output and Data Communications]: Data Communications Device; I.4.1 [Image Processing and Computer Vision]: Digitization and Image Capture—*sampling, scanning*

### Keywords

visible light communication (VLC), spatial light modulator (SLM), MIMO, imaging receiver

## 1 Introduction

Like MIMO radio-frequency (RF) communication systems, visible light communication (VLC) systems can use multiple transmitters and receiver elements to increase the capacity of their wireless communication links. Unlike MIMO RF systems though, the line-of-sight components tend to dominate over the multipath components in MIMO VLC systems [14]. In the absence of significant fading due to random multipath signal propagation, the channel gain

from each transmitter to each receiver element can be approximated as a deterministic function of the relative positions and orientations of the transmitter and receiver (assuming that the line-of-sight is not obstructed).

The deterministic and position-dependent nature of VLC channel gains presents both potential advantages and practical disadvantages. On one hand, MIMO VLC systems cannot rely on random channel gains from rich scattering environments to provide the well-conditioned channel matrices needed for MIMO communication systems to perform well. This problem is illustrated in the work of Zeng et. al., which shows that the bit error rate (BER) becomes unacceptably high for a non-imaging VLC system whenever the transmitters are positioned symmetrically about the VLC receiver [14].

On the other hand, the negligible random multipath signal propagation yields a more predictable VLC channel. This predictability presents opportunities to deliberately engineer the VLC channel to improve the resulting MIMO channel capacity.

In this paper, we introduce a new MIMO VLC receiver architecture that includes a built-in spatial light modulator (SLM). This built-in SLM enables the VLC receiver to dynamically adjust the optical communication channel to better adapt to changing transmitter and receiver positions in mobile use cases. As a result, the MIMO VLC receiver requires fewer photodetectors to receive reliably in mobile use cases.

Section 2 presents background. Section 3 introduces the SLM MIMO VLC receiver and details its operation. Section 4 presents the channel model for the SLM VLC receiver. Section 5 presents the preliminary procedures and algorithms for controlling the proposed receiver. Section 6 compares the performance of the proposed receiver against other imaging VLC receivers. And section 7 concludes the paper.

## 2 Background

In the high SNR regime, MIMO communication systems aim to maximize the rank and minimize the condition number of the channel matrix in order to improve the multiplexing capacity gains [10, p. 294–295]. Two general classes of MIMO VLC receivers have been previously proposed for this purpose: imaging VLC receivers [14, 1, 3, 13, 2, 7] and non-imaging VLC receivers [11, 6, 12]. Although both

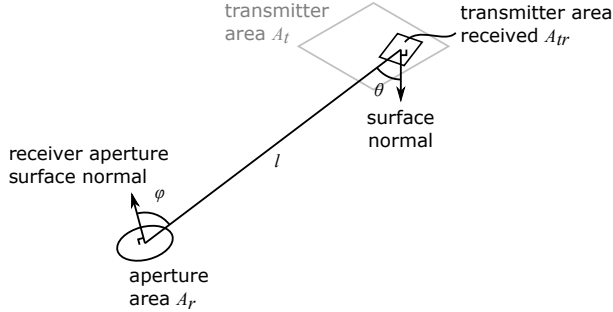


**Figure 1. Parameters used in equation 1 to calculate the gain from a uniformly diffuse transmitter to an imaging receiver pixel.**

types of MIMO VLC receivers can yield full-rank and well-conditioned channel matrices when the transmitters are sufficiently separated from each other, these receivers may yield poorly conditioned channel matrices when the transmitters are close to each other.

For example, the gain from a uniformly diffuse (Lambertian) transmitter to an imaging receiver pixel is

$$\frac{P_r}{P_t} = \frac{A_{tr}A_r}{\pi A_t l^2} \cos \theta \cos \phi \quad (1)$$

where  $A_r$  is the area of the imaging receiver's aperture,  $A_{tr}$  is the transmitter seen by the pixel,  $A_t$  is the total area of the transmitter's uniformly diffuse emitting surface,  $l$  is the distance between the transmitter and the receiver's aperture,  $\theta$  is the angle between the normal of the transmitter's surface and the straight path from the transmitter to the receiver,  $\phi$  is the angle between the normal of the receiver's aperture and the straight path from the transmitter to the receiver,  $P_t$  is the transmitted optical power, and  $P_r$  is the received optical power.<sup>1</sup> If two transmitters are close enough that their optical signals are entirely received by the same imaging receiver pixels, then the position-dependent parameters ( $l, \theta, \phi, A_{tr}$ ) would be approximately equal between the two transmitters. Thus, the corresponding columns of the channel matrix would be approximately equal, resulting in a poorly conditioned channel matrix.

In mobile use cases, this situation may arise if the transmitters are allowed to move near each other or if the receiver is oriented to receive from transmitters that are farther away. Although this problem can be mitigated by increasing the number of pixels in the imaging VLC receiver to reduce the likelihood that signals from neighboring transmitters are received by the same pixels [2], adding additional pixels may require compromises in pixel sensitivity, sampling rate, power consumption, cost, and device size.

Similarly for the non-imaging VLC receivers [11, 6, 12], the channel gains to the receiver elements also vary gradually with respect to the relative position and orientation of the transmitters. When the transmitters are positioned close to

<sup>1</sup>Derived from [5, ch. 3] assuming only path loss, assuming that neither the transmitter nor the receiver are facing away from each other, assuming no blur in the transmitter's image, and assuming that the transmitters and receivers are small relative to the distance between them.

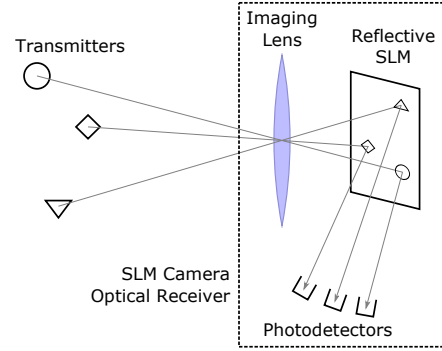


**Figure 2. A MIMO VLC system using the SLM Camera Optical Receiver is shown. In this system, an imaging lens focuses light from multiple transmitters onto a reflective SLM that redirects the light from each transmitter to a separate photodetector.**

each other, the corresponding columns of the channel matrix would be similar, resulting in a poorly conditioned channel matrix.

### 3 Imaging SLM VLC receiver

The proposed MIMO VLC receiver architecture is an imaging receiver architecture that replaces the traditional image sensor (i.e., photodetector array) with a spatial light modulator (SLM). Unlike traditional imaging receivers, the SLM at the image plane (where the images of the transmitters are focused) do not measure the incoming optical signal. Rather, the SLM redirects the light towards a separate array of photodetectors to be measured, which are not located on the image plane.

#### 3.1 Structure of the Receiver

As shown in figure 2, this SLM Camera Optical Receiver (SLMCOR) consists of an imaging lens, a reflective SLM, and multiple photodetectors; implementations would also require signal processing and control devices, which are shown in figure 5. Although a variety of SLMs can be used in an imaging SLM VLC receiver, to simplify the description of the architecture, this paper assumes that the SLM is a reflective SLM that consists of a rectangular array of flat micromirrors. Each micromirror can be rotated in place across a range of angles and each mirror in the array can be independently controlled. By varying the orientation of a pixel's micromirror, the SLM can control the reflection angle of the light incident on the pixel, and thus, aim the reflected light towards a selected photodetector.

The photodetectors are arranged around the SLM, facing the SLM, so that each SLM micromirror can redirect light towards any of the photodetectors.

This setup is similar to (and in part, inspired by) the "single-pixel" camera by Duarte et. al. [4]. By separating the photodetector(s) from the image plane, where image formed by the imaging lens is focused, the architecture enables the imaging system to have very high resolution with very few photodetectors. This capability allows us to avoid the practical tradeoffs between the quantity of photodetectors and the performance of each photodetector.

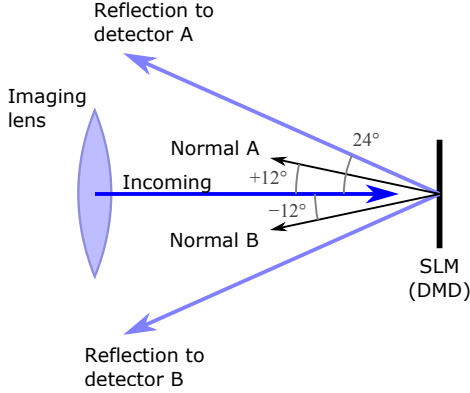


**Figure 3.** Since each micromirrors can each rotate  $\pm 12^\circ$  and the reflected beam is deflected by  $24^\circ$  in either direction. The photodetectors should be positioned at  $\pm 24^\circ$  to detect the reflected beams.

However, our proposed receiver also differs from the single-pixel camera in significant ways to greatly improve the receiver’s sampling rate for high-speed signals. One difference is that our receiver uses more than one photodetector—we use one for each transmitter—to sample signals from multiple transmitters simultaneously. Furthermore, as detailed in subsection 5, SLMCOR uses different SLM patterns generated by different algorithms that use feedback from the received VLC signals.

### 3.2 2x2 MIMO Prototype

The SLMCOR was implemented using a Texas Instruments (TI) digital micromirror device (DMD) from the DLP LightCrafter 6500 evaluation kit [8] as the reflective SLM. This DMD has an array of 1920 by 1080 (1080p resolution) micromirrors that are flat in the “reset” state. Each micromirror can be independently rotated about its diagonal to one of two angles: either  $+12^\circ$  or  $-12^\circ$  [9]. Since the each micromirror can take one of two possible positions (and cannot be independently configured to rotate to any other position), the micromirrors can be used to select between two photodetectors to receive the light. These two photodetectors are positioned at  $+24^\circ$  and  $-24^\circ$  as shown in figure 3.

Since each micromirror rotates about its diagonal, the DMD was rotated  $45^\circ$  about its normal vector to align the reflected beams with the photodetector on the optical-breadboard implementation shown in figure 4.

As labeled in figure 4, the DLP SLMCOR uses three lenses: one concentrator lens for each photodetector and the main imaging lens. The main imaging lens is a 25.4 mm diameter biconvex lens with a focal length of 50.0 mm from Thorlabs (part number LB1471-A). For DMD’s image area of 14.52 mm by 8.16 mm [9], this relatively long focal length unfortunately yields a relatively narrow field of view of approximately  $16.5^\circ$  by  $9.3^\circ$  (full angle). Although a shorter focal length would provide a wider field of view (enabling the receiver to receiver from transmitters in a wider range of positions), we were unable to accommodate a shorter focal length using commercially-available off-the-shelf (COTS) lens holders without obstructing the reflected beams from the DMD. Future revisions of this prototype may be able to im-

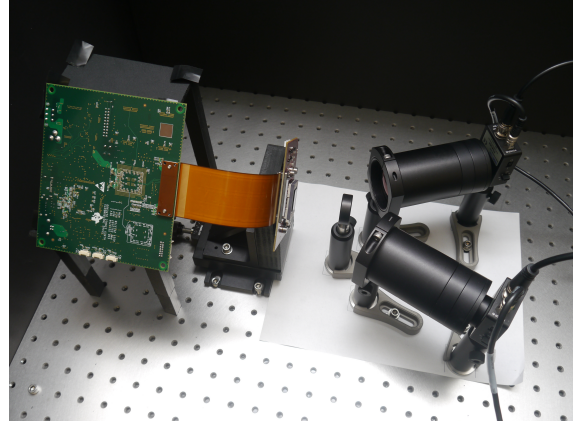


**Figure 4.** The 2-photodetector SLMCOR prototype using a TI DLP as the SLM.

prove the FoV, optical gain, and size of the VLC receiver by using custom lenses and optomechanical components.

Another consideration in selecting the main imaging lens was the lens diameter. Although larger lens would enlarge the aperture over which the receiver gathers light, thus improving the receiver’s optical gain, enlarging the aperture would also widen the beam angle for both the light focused onto the DMD and the light reflected from the DMD. Given that the central ray of the reflected beam is offset  $24^\circ$  from the imaging lens’s optical axis, the beam half-angle should not exceed  $12^\circ$ ; otherwise, a portion of the reflect beam will be directed back towards the main imaging lens, where it cannot be detected by a photodetector.

The prototype uses two Thorlabs PDA36A photodetectors. Since each photodetector’s body is relatively large, they are positioned further away to avoid blocking light from the main imaging lens to the DMD. A Thorlabs LB1723-A 50.8 mm diameter lens is placed in front of each photodetector to focus the reflected beams onto the photodetector.

Zemax was used to perform ray-tracing simulations to adjust the focus of the lenses and the placement of the photodetectors.

## 4 SLM VLC receiver channel model

Applying the small-signal approximation, we make the simplifying assumption that the received shot noise is independent of the transmitted signals. Using this assumption, when the system has  $n_t$  transmitters,  $n_r$  photodetectors, and  $n_s$  SLM pixels, the channel can be modeled as

$$\mathbf{y} = \mathbf{S}(\mathbf{H}\mathbf{x} + \mathbf{w}_s) + \mathbf{w}_t \quad (2)$$

where  $\mathbf{x} \in \mathbb{R}^{n_t}$  represents the transmitted signal,  $\mathbf{y} \in \mathbb{R}^{n_r}$  represents the received signal,  $\mathbf{w}_s \in \mathbb{R}^{n_s}$  represents the shot noise contribution of each SLM pixel (e.g., due to background illumination),  $\mathbf{w}_t \in \mathbb{R}^{n_r}$  represents the thermal noise for each photodetector,  $\mathbf{H} \in \mathbb{R}^{n_s \times n_t}$  represents the gain from each transmitter through each SLM pixel to a photodetector, and  $\mathbf{S} \in \mathbb{R}^{n_r \times n_s}$  represents the fraction of optical power incident on each SLM pixel that is distributed to each photodetector. For the 2-photodetector DLP-based SLM VLC receiver,  $n_r = 2$  and  $n_s = 1920 * 1080 = 2.0736 * 10^6$ .

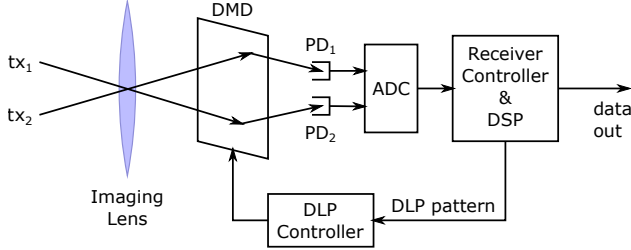


**Figure 5. A block diagram of the 2-PD DLP SLM VLC receiver showing the control loop and signal chain.**

Effectively, the resulting channel matrix, representing the gain from each transmitter to each receiver, is

$$\mathbf{G} = \mathbf{S}\mathbf{H} \quad (3)$$

where  $\mathbf{G}$  is a  $n_r$  by  $n_t$  matrix. By controlling the pattern shown by the DMD, controls  $\mathbf{S}$ , and is thus able to adjust the resulting channel matrix. For simplicity, we assume that each micromirror directs all of its light towards one selected photodiode. Thus, each column of  $\mathbf{S}$  has exactly one non-zero element in the row representing the selected photodiode and the non-zero element is exactly equal to one.

For the purpose of modeling shot noise (in  $\mathbf{w}_s$ ), we apply the simplifying assumption that the shot noise variance is identical across all SLM pixels. We further approximate the shot noise, which is actually due to a Poisson process, as additive white Gaussian noise (AWGN).

The elements of  $\mathbf{w}_t$  are also modeled as independent and identically-distributed AWGN. We neglect other sources of noise.

## 5 Operation of the 2-PD SLMCOR

In addition to decoding the received signal, SLM VLC receivers should also configure the SLM to obtain a useful channel matrix. This configuration is orchestrated by the receiver controller using feedback from the received VLC signals as illustrated in figure 5. For the DMD in the 2-photodetector (PD) DLP-based SLM VLC receiver, the receiver controller configures the DMD by sending the DLP controller a bitmap image consisting of 1920 by 1080 pixels. Each pixel in the image specifies the orientation of the corresponding micromirror in the DMD: a dark pixel orients the corresponding micromirror to direct light towards one photodetector while a bright pixel orients the micromirror to direct light towards the other photodetector. In turn, the DLP controller generates the appropriate electrical signals to move the micromirrors in the DMD. In this paper, we refer to an instance of this SLM configuration as a “pattern”.

The generation of SLM patterns can be split into three sub-problems: initially measuring  $\mathbf{H}$ , generating the appropriate SLM pattern given  $\mathbf{H}$ , and tracking the transmitters as they move relative to the receiver. We present preliminary solutions to these sub-problems for a proof-of-concept. Future strategies will likely further improve the performance of the SLM VLC receiver.

### 5.1 Initially measuring $\mathbf{H}$

As explained in section 4, the resulting channel matrix is determined by both  $\mathbf{S}$  and  $\mathbf{H}$ . To optimize the channel ma-

trix, the receiver controller first measures  $\mathbf{H}$ : the gain from each transmitter to a photodetector through each SLM. For simplicity, we assume that this gain is the same for either photodetectors.

To facilitate transmitter-to-photodetector gain measurements, to enable the receiver to identify which transmitter transmitted any signal, and to facilitate the tracking of transmitters as they move relative to the receiver, we propose allocating a small portion of the available bandwidth for each transmitter to embed a continuously-transmitted unique identification signal of a known amplitude. At the receiver, the identification signal can be isolated by filtering to pass the identification band, and (assuming that gain of the identification signal is representative of the gain at other frequencies) the gain can be determined by dividing the amplitude of the received identification signal by the amplitude of the transmitted identification signal.

To ensure that the identification signals can be separated from each other in case of interference between multiple transmitters, the unique identification signals should be orthogonal to each other. This orthogonality can be achieved by selecting  $m_t$  evenly spaced frequencies within the identification band as the unique identification signals, where  $m_t$  is the maximum supported number of active transmitters that can be in the receiver’s field of view. Assuming that  $\mathbf{H}$  varies very slowly (compared to the VLC symbol rate), these identification symbols can be sampled over long periods of time, allowing the receiver to finely resolve differences in frequency. As a result, the identification band can have a very narrow bandwidth, and thus, reserving this band for identification and channel-state measurements would not significantly decrease the capacity of the system.

The transmitter-to-photodetector gain through each pixel can be measured by first splitting the pixel array in half, directing half of the pixels toward photodetector 1 (PD1) and the other half toward photodetector 2 (PD2). The signals received by both photodetectors are checked for the presence of a transmitter’s identification signal (that is significantly above the noise floor). If no identification signal is found, then the rows of  $\mathbf{H}$  corresponding to those pixels are 0. The process is then repeated recursively for each partition of pixels that do receive an identification signal, splitting the partition in half and using just PD1 to sample one sub-partition at a time (since all other pixels must be directed toward PD2), until the partition is just one pixel. When the partition consists of just one pixel, the originating transmitter and gain of the signal that is received by the pixel can be determined by measuring the identification signal as described above.

Future protocols may be able to further reduce the time needed to initially measure  $\mathbf{H}$ .

### 5.2 Generating the SLM pattern

Given  $\mathbf{H}$ , the receiver controller can determine how many active transmitters are in the receiver’s field of view and which transmitter images are incident on which SLM pixel.

If only one transmitter is in the field of view, the receiver controller can generate a SLM pattern to eliminate shot noise from the pixels that do not receive from that transmitter by directing those pixels toward PD2 and directing the pixels that do receive from the transmitter towards PD1. In this

scenario, the SLM VLC receiver performs selection diversity combining in this single-input and multiple-output (SIMO) system.

If two transmitters are in the field of view, pixels receiving signals from the first transmitter can be directed towards PD1 and pixels receiving signals from the second transmitter can be directed towards PD2. Pixels that receive from both transmitters can be directed based on which transmitter has a greater gain through that pixel. Since the DMD must direct light towards one of the two photodetectors, the remaining pixels that receive no VLC signal and only contribute to shot noise can be directed toward the photodetector receiving the signal with the highest SNR.

The 2-PD DLP SLM VLC receiver cannot simultaneously receive from more than two transmitters due to the limited number of photodetectors. However, if more than two transmitters are available, the additional transmitters can be configured to transmit the same signals as one of the two transmitters (i.e., beamforming).

### 5.3 Tracking the transmitters

Except when no transmitters were previously detected, neither photodetectors are free to update the measurements of  $\mathbf{H}$  after initialization. To update a row of  $\mathbf{H}$  after initialization, first, measure the amplitude of each identification signal received by both photodetectors. Since the identification signals are continuously transmitted, this measurement can be done without interrupting data transmission.

Then, toggle the corresponding DMD pixel for that row so that the pixel switches from one photodetector to the other. We assume that the resolution is sufficiently high that changing one pixel will not significantly increase the probability of error. After toggling the pixel, measure the amplitude of each identification signal received by both photodetectors again.

Assuming that no other event altered the transmitter-to-photodetector gains during this procedure, the change in amplitude of each identification signal is entirely due to the toggled pixel. Thus, the difference in amplitude of each identification signal can be treated as the incremental contribution of the pixel, and can be used to calculate the gains through that pixel by dividing this incremental contribution by the amplitude of the identification signals at the transmitter.

The receiver may prioritize updating  $\mathbf{H}$  for pixels nearest to the boundaries of the DMD and of the transmitter images to better track transmitters as they move incrementally or as they enter the field of view.

## 6 Performance

We compare the 2-photodetector DLP-based imaging VLC receiver against traditional imaging VLC receivers with 2, 4, and 9 photodetectors to illustrate the advantage of the DLP-based imaging receiver. In this comparison, we simulate each of the receivers with two pseudo-randomly positioned transmitters in the receiver's field of view to determine the average channel matrix rank and median channel matrix condition number. These two metrics (the rank and condition number) indicate the capacity of the MIMO channel in the high SNR regime [10, p. 294–295].<sup>2</sup> We use the median

<sup>2</sup>Although the RF channel model used in [10] differs in significant ways from VLC channels (e.g., VLC signals are non-negative and may not be

**Table 1. Simulation results comparing average rank and median condition number.**

	Average rank	Median condition number
DLP SLM	2.0	1.01
2-pixel	1.7	1.14
4-pixel	1.9	1.10
9-pixel	1.9	1.23

condition number instead of mean condition number as the metric because the condition number may be infinite.

To isolate and highlight the effects of adding a SLM, we use the same optical system parameters for both the DLP-based and the traditional imaging VLC receiver:

**Aperture radius** 25.4 mm

**Lens to array distance** 49.9 mm

**Pixel array width** 14.52 mm

**Pixel array height** 8.16 mm

**Receiver position** (0,0,0) (imaging lens at origin)

**Receiver zenith angle** 0° (in the +z-axis direction)

**Transmitter shape** 40 mm by 40 mm (square)

**Transmitter position**  $z = 2.5$  m

**Transmitter orientation** downward

For each imaging receiver, the pixels are uniform in size and tiled to cover the entire area of the pixel array without overlap (for a 100% fill factor).

In each of the 10 trials simulated to obtain the mean rank and median condition number, the centers of the two transmitters are uniformly distributed within the receiver's field of view on the plane at  $z = 2.5$  m.

To determine where each transmitter's image lands on the receiver's pixel array, we assume that the imaging receiver is perfectly in focus, and apply the paraxial thin-lens approximation. With this simplification, the transmitter image lands where the ray from the transmitter that goes through the center of the imaging lens intersects with the image plane. Conversely, the portion of the transmitter seen by a pixel can be determined by projecting each vertex of the pixel's polygon as a ray from the pixel through the center of the imaging lens to the transmitter's plane (at  $z = 2.5$  mm) as illustrated in figure 2.

Given this projected pixel polygon on the transmitter's plane, equation 1 can be used to determine the gain from each transmitter to each pixel. For this comparison, we assume that the transmitter-to-pixel gain equals the gain from the transmitter to a photodetector through that pixel.  $A_{TP}$  can be determined as the area of the intersection between the transmitter polygon and the projected pixel polygon. We assume that each pixel is sufficiently small that  $l$ ,  $\theta$ , and  $\phi$  does not vary significantly over the area of the pixel.

The simulation results are highlighted in table 1. A higher rank and a condition number closer to one indicates better MIMO performance in the high SNR regime. The simulation results show that the 2-photodetector DLP SLM VLC

Gaussian distributed), we assume that these metrics remain sufficiently valid for a rough comparison between VLC systems.

receiver is able to significantly out-perform the traditional imaging VLC receivers even when the traditional imaging VLC receivers use more photodetectors. Note that additional digits are shown for the median condition number to show that the condition number is not perfect for the DLP SLM.

## 7 Conclusion

MIMO VLC systems differ from MIMO RF systems in significant ways. Due to a lack of multipath signal propagation, VLC channel gains depend strongly on the relative positions of the transmitters with respect to the receiver and do not vary significantly from random fading. As a result, the VLC system may perform poorly whenever the transmitters and receiver are in certain positions; in the absence of random fading over time, these poor channel conditions may persist until the transmitters or receiver moves. These dead spots limit the utility of MIMO VLC systems for mobile use cases.

In this paper, we propose a new MIMO VLC receiver architecture that can dynamically alter the channel matrix using a spatial light modulator to both avoid dead spots and to enhance the performance of the resulting channel. By taking advantage of the relatively slow-changing nature of VLC channel gains, the proposed VLC receiver can measure and adjust the channel matrix to improve SNR and track transmitters as they move relative to the receiver.

Although the current DLP-based SLM VLC receiver can only support two photodetectors, we demonstrate through simulations that the SLM VLC receiver still outperforms imaging VLC receivers that have more photodetectors in terms of channel matrix rank and condition number. In future work, we aim to increase the number of photodetectors that can be supported by the SLM VLC receiver, refine our preliminary algorithms for controlling the VLC receiver, validate our simulation results through our physical prototype, and develop better metrics to compare VLC receivers.

## 8 Acknowledgment

This work was supported primarily by the Engineering Research Centers Program of the National Science Foundation under NSF Cooperative Agreement No. EEC-0812056.

## 9 References

- [1] A. Azhar, T.-A. Tran, and D. O'Brien. Demonstration of high-speed data transmission using MIMO-OFDM visible light communications. In *GLOBECOM Workshops (GC Wkshps)*, 2010 IEEE, pages 1052–1056, 2010.
- [2] J. C. Chau and T. D. Little. Scalable imaging VLC receivers with token-based pixel selection for spatial multiplexing. In *Proceedings of the 1st ACM MobiCom Workshop on Visible Light Communication Systems*, VLCS '14, pages 21–26, New York, NY, USA, 2014. ACM.
- [3] K. Dambul, D. O'Brien, and G. Faulkner. Indoor optical wireless MIMO system with an imaging receiver. *Photonics Technology Letters*, IEEE, 23(2):97–99, Jan. 15, 2011.
- [4] M. Duarte, M. Davenport, D. Takhar, J. Laska, T. Sun, K. Kelly, and R. Baraniuk. Single-pixel imaging via compressive sampling. *Signal Processing Magazine, IEEE*, 25(2):83–91, 2008.
- [5] N. S. Kopeika. *A System Engineering Approach to Imaging*. SPIE Optical Engineering Press, 1998.
- [6] A. Nuwanpriya, S.-W. Ho, and C. S. Chen. Angle diversity receiver for indoor MIMO visible light communications. In *Globecom Workshops (GC Wkshps)*, 2014, pages 444–449, Dec 2014.
- [7] S. Rajbhandari, H. Chun, G. Faulkner, D. O'Brien, A. V. N. Jalajakumari, K. Cameron, R. Henderson, E. Xie, J. J. D. McKendry, J. Hermsdorf, E. Gu, M. D. Dawson, D. Tsonev, M. Ijaz, and H. Haas. Multi-gigabit integrated MIMO visible light communication system: Progress and updates. In *Proceedings of IEEE Photonics Summer Topicals*, pages 230–231, 2015. Proceedings from CD; update BibTeX entry when it's available online.
- [8] Texas Instruments. *DLP LightCrafter 6500 and 9000 EVM User's Guide*, December 2014. Literature Number: DLP028A.
- [9] Texas Instruments. *DLP6500FYE DMD*, October 2014. DLPS053.
- [10] D. Tse and P. Viswanath. *Fundamentals of Wireless Communication*. Cambridge University Press, 2005.
- [11] T. Wang and J. Armstrong. Performance of indoor MIMO optical wireless system using linear receiver with prism array. In *Communications Theory Workshop (AusCTW)*, 2014 Australian, pages 51–56, Feb 2014.
- [12] T. Wang, C. He, and J. Armstrong. Angular diversity for indoor MIMO optical wireless communications. In *Communications (ICC)*, 2015 IEEE International Conference on, pages 5066–5071, June 2015.
- [13] T. Q. Wang, Y. A. Sekercioglu, and J. Armstrong. Hemispherical lens based imaging communication MIMO optical wireless communications. In *3rd IEEE Workshop on Optical Wireless Communications (OWC'12)*, pages 1239–1243, Dec 2012. Can't find online; from Litle.
- [14] L. Zeng, D. O'Brien, H. Minh, G. Faulkner, K. Lee, D. Jung, Y. Oh, and E. T. Won. High data rate multiple input multiple output (MIMO) optical wireless communications using white LED lighting. *Selected Areas in Communications, IEEE Journal on*, 27(9):1654–1662, December 2009.